Aschamalmite (Pb$_6$Bi$_2$S$_9$): crystal structure and ordering scheme for Pb and Bi atoms

A. M. CALLEGARI[1] AND M. BOIOCCHI[2]

[1] Dipartimento di Scienze della Terra, Università degli Studi di Pavia, via Ferrata 1, I-27100 Pavia, Italy
[2] Centro Grandi Strumenti, Università degli Studi di Pavia, via Bassi 21, I-27100 Pavia, Italy

ABSTRACT

The first single-crystal structure refinement of aschamalmite (Pb$_6$Bi$_2$S$_9$) from Susa Valley (Piedmont, Italy) is reported. The mineral is monoclinic, $C2/m$, a = 13.719(1) Å, b = 4.132(1) Å, c = 31.419(3) Å, β = 90.94(1)º, V = 1 780.8(4) Å^3, Z = 4. The Pb$_6$Bi$_2$S$_9$ compound crystallizes also in an orthorhombic form as heyrovskyite (*Cmcm*) and our study is focused on understanding the reason leading to a change in symmetry. The aschamalmite structure forms because of ordering between Pb and Bi on the margins of the two octahedral layers that are symmetrically equivalent in heyrovskyite. The two alternate set of octahedral slabs are not related by a crystallographic mirror plane and the symmetry decreases to monoclinic. The cation ordering couples opposite sequences of Pb and Bi octahedra at the margins of slabs. In particular, the succession $^{[Me4A]}$Bi-$^{[Me5A]}$Pb-$^{[Me4A]}$Bi-$^{[Me5A]}$Pb faced to the series $^{[Me4B]}$Pb-$^{[Me5B]}$Bi-$^{[Me4B]}$Pb-$^{[Me5B]}$Bi occurs in about 70% of the unit-cells of the crystal, while the contrary sequence ($^{[Me4A]}$Pb-$^{[Me5A]}$Bi-$^{[Me4A]}$Pb-$^{[Me5A]}$Bi faced to $^{[Me4B]}$Bi-$^{[Me5B]}$Pb-$^{[Me4B]}$Bi-$^{[Me5B]}$Pb) occurs in the remaining unit-cells. The marginal octahedra have ideal populations (a.p.f.u.): $^{[Me4A]}$1.40Bi+0.60Pb, $^{[Me4B]}$1.40Pb+0.60Bi, $^{[Me5A]}$1.40Pb+0.60Bi, $^{[Me5B]}$1.40Bi+0.60Pb, in agreement with our structure-refinement results.

The probable site populations for pure heyrovskyite have been proposed, as well as the reasons that prevent the formation of a completely ordered monoclinic phase.

Introduction

ASCHAMALMITE is a rare sulphosalt with the ideal formula Pb$_6$Bi$_2$S$_9$. It was described for the first time by Mumme *et al.* (1983), who found the mineral in a leucocratic albite-gneiss from Ascham Alm in the Untersulzbach Valley in Austria. Aschamalmite was associated with several other sulphates and sulphosalts, and sulphides such as pyrrhotite, chalcopyrite, pyrite, galena, galenobismutite and friedrichite.

Aschamalmite is considered to be the mono-clinic form of the compound Pb$_6$Bi$_2$S$_9$, which is also the chemical formula of the orthorhombic mineral heyrovskyite. Both minerals are members of the ^{7,7}L lillianite homologue series (Moëlo *et al.*, 2008). Mumme *et al.* (1983) suggested that aschamalmite was not a dimorph of heyrovskyite *sensu strictu* because the latter always contained a significant amount of monovalent Ag and a corresponding extra Bi content (Bi >2 a.p.f.u.) for charge balance. However, heyrovskyite crystals free of Ag were subsequently found at Vulcano, Aeolian Islands, Italy (Borodaev *et al.*, 2003).

The crystal structure of Ag-bearing heyrovs-kyite was previously described (Takeuchi and Takagi, 1974; Makovicky *et al.*, 1991), but the crystal structure of aschamalmite has never been studied in detail. Crystallographic data reported by Mumme *et al.*, (1983) established that aschamalmite was monoclinic and suggested

that its crystal structure was strictly related to heyrovskyite, the two unit cells being very similar. Consequently, aschamalmite was considered as a 'monoclinic heyrovskyite' form. The change in symmetry, from orthorhombic (*Cmcm*) to monoclinic (*C2* or *Cm* or *C2/m*), was ascribed to ordering between Pb and Bi species at the octahedral sites. However, the crystal-structure refinement of aschamalmite was not reported and the structural data were not known.

Recently, aschamalmite samples have been found in phengitic gneiss at the Susa Valley, Piedmont, Italy (Callegari *et al.*, 2008). This is the third discovery of this rare mineral in Italy. It was found previously at the Ossola Valley (Perchiazzi, 1989) and at Costabella mine, near Savona, Liguria (Balestra and Armellino, 2001). Millimetre-sized dark aschamalmite crystals with lamellar habit are contained in a colourless matrix of K-feldspar, quartz and phengitic mica (Fig. 1). No other mineral species are present in the samples we studied.

These new samples of aschamalmite produced an X-ray diffraction (XRD) pattern of a quality suitable for single-crystal data collection and our work reports the first structure refinement, the aim being to clarify the distribution of Bi and Pb among all available sites and to describe the crystal-chemical reasons leading to the change in symmetry.

Experimental procedures

Single-crystal XRD study

Diffraction data were collected from a very small platy-grey crystal by means of a Bruker-AXS three circle diffractometer, equipped with the Smart-Apex CCD detector. Omega rotation frames were processed by the *Saint* software (Bruker, 2003) and intensity data were corrected for background, Lorentz and polarization effects. Absorption effects were evaluated by an empirical method (*SADABS*; Sheldrick, 1996) and an absorption correction was applied to the data.

FIG. 1. Grey lamellar aschamalmite sample from Susa Valley enclosed in a quartz and K-feldspar matrix. The lamella is about 20 mm × 2 mm in size.

Details of the single-crystal diffraction study are reported in Table 1.

Systematic absences were compatible with the $C2$, Cm and $C2/m$ space groups, whereas the $|E^2-1|$ value (1.06) strongly suggested the existence of the centre of inversion. Therefore, the $C2/m$ space group was chosen and the crystal structure was solved by direct methods (*SIR97*; Altomare *et al.*, 1999). The crystal structure thus solved confirmed the strong structural similarity with heyrovskyite and, for a better comparison, the heyrovskyite of Makovicky *et al.* (1991) was transformed into the *Ccmm* space group. In this way, both unit cells had the same orientation and the atom sites of aschamalmite were labelled starting from those of heyrovskyite by adding the A and B suffix to the corresponding mirror-related atoms. In particular, in aschamalmite there are two independent slabs because of the absence of the (001) mirror plane passing through the Me1 polyhedron.

Anisotropic crystal-structure refinement was performed with a locally-modified version of the program *ORFLS* (Busing *et al.*, 1962) with unitary weight using reflections with $F_{obs}>3\sigma(F_{obs})$. Scattering curves for neutral chemical species were used. However, direct occupancy refinement failed because the Pb and Bi are almost isoelectronic and the cation site population was consequently assigned on the basis of geometrical features (see below). Atomic coordinates are listed in Table 2 and selected bond distances and bond angles in Table 3. Anisotropic displacement parameters are deposited with the Principal Editor of *Mineralogical Magazine* and are available from: www.minersoc.org/pages/e_journals/dep_mat_mm.html.

Chemical analysis

The same crystal used for XRD was investigated by means of electron microprobe analyses, performed with a Cameca SX 50 instrument. A preliminary EDS analysis showed that only Pb, Bi and S were present and the complete WDS analysis was performed using a focused beam of ~1 μm diameter. For the analysis of Pb, a gun potential of 15 kV and a probe current of 15 nA was used; for Bi and S, 20kV and 15 nA respectively. The following probe standard and emission lines were used: PbTe (Pb-$M\alpha$), metallic bismuth (Bi-$M\alpha$) and pyrite (S-$K\alpha$).

From eight point analyses, the following mean values (wt.%) were obtained: Pb 63.55±0.40; Bi 21.27±0.14; S 14.79±0.10; total = 99.61. The resulting formula: $Pb_{5.99}Bi_{1.99}S_9$ confirms the stoichiometry of the sample.

Results

The crystal structure of aschamalmite

The crystallographic study confirms that aschamalmite is a $^{7,7}L$ homologue of the lillianite series, and the general set of alternate slabs is shown in Fig. 2. Sulphosalts of this accretional series have crystal structures consisting of alternate sets of PbS-like modules of various thickness, cut parallel to $(311)_{PbS}$ and converging towards a bicapped trigonal prism PbS_{6+2} (Makovicky, 1977; Makovicky and Karup-Møller, 1977a,b; Makovicky and Balić-Žunić, 1993). Each different homologue is identified by the code: $^{N1,N2}L$; where *N1* and *N2* are the number of octahedra (L) which form the two types of slabs. Normally, when *N1* and *N2* have the same value, the adjacent layers of octahedra are related

TABLE 1. Crystal data for aschamalmite.

Crystal size (mm)	$0.070 \times 0.020 \times 0.008$
a (Å)	13.719(1)
b (Å)	4.132(1)
c (Å)	31.419(3)
β (°)	90.94(1)
V (Å^3)	1780.8(2)
Z	4
Space group	$C2/m$
Detector type	CCD plate
Wavelength (Å)	0.71073
μ (cm^{-1})	77.26
Sample to detector distance (mm)	70
Scan mode	ω
Scan width (°)	0.2
Acquisition time (s)	50
No. collected F	12138
No. unique F	2932
No. Obs. F ($I/\sigma(I) \geqslant 3$)	2141
2θ range (°)	4−60
h, k, l range	±19, ±5, ±44
Completeness (%)	99.7
Mean redundancy	4.13
R_{sym} (%)	0.042
R_{obs} (%)	0.064
R_{all} (%)	0.084

TABLE 2. Fractional atom coordinates and equivalent isotropic displacement parameters (estimated standard deviations in parentheses).

Atom	x/a	y/b	z/c	U_{eq} (Å^2, $\times 10^4$)
Me1	0.4215(1)	0	0.2462(1)	364(7)
Me2A	0.5	0	0	149(6)
Me2B	0.5	0	0.5	145(6)
Me3A	0.2298(1)	0	0.0580(1)	163(4)
Me3B	0.2279(1)	0	0.4419(1)	152(4)
Me4A	0.6883(1)	0	0.1749(1)	175(4)
Me4B	0.6773(1)	0	0.3253(1)	172(4)
Me5A	0.9601(1)	0	0.1188(1)	163(4)
Me5B	0.9523(1)	0	0.3803(1)	140(4)
S1A	0.0552(6)	0	0.1948(3)	205(28)
S1B	0.0381(6)	0	0.3047(3)	249(31)
S2A	0.5891(6)	0	0.0858(3)	198(27)
S2B	0.5812(5)	0	0.4132(3)	199(27)
S3	0.7814(5)	0	0.2491(3)	195(27)
S4A	0.3291(5)	0	0.1474(3)	213(29)
S4B	0.3240(6)	0	0.3564(3)	232(30)
S5A	0.8614(5)	0	0.0265(3)	192(27)
S5B	0.8600(5)	0	0.4718(3)	161(24)

by a mirror plane passing through the intermediate bicapped trigonal prisms.

Aschamalmite and heyrovskyite are the only two known members of the ^{7,7}L group.

In particular, the structure of aschamalmite (space group $C2/m$) is shown in Fig. 3a to contain nine independent cation sites (Me1, Me2A, Me2B, Me3A, Me3B, Me4A, Me4B, Me5A, Me5B). Me1 is the bi-capped trigonal prism towards which converge the two alternate set of PbS-like slabs arranged in accordance with the presence of a pseudo-mirror plane normal to the c axis. The first slab is formed by octahedral sites with the A suffix and the second slab is formed by octahedral sites with the B suffix.

Conversely, heyrovskyite (Ccmm) has the alternate set of slabs related by a mirror plane normal to the c axis (Fig. 3b) and its structure is formed by an independent Me1 site (on the mirror plane) and by only four independent octahedral sites (Me2, Me3, Me4, Me5).

In detail, both minerals have the middle portions of octahedral layers formed by octahedra (Me2 and Me3 in heyrovskyite, the same atom names with the A and B suffix in aschamalmite) that share all their edges with other octahedra (as in galena). The marginal portions are formed by octahedra that share only seven (Me4) and ten (Me5) edges with other octahedra. Two Me4 octahedra in heyrovskyite, and the octahedral couples Me4A and Me4B

TABLE 3. Bond lengths (Å), selected bond angles (º), polyhedral volumes (Å^3) and octahedral angle variance − OAV (^{o2}) in aschamalmite.

$Me1-S1A^{5,7}$ ×2	3.215(8)
$Me1-S1B^{5,7}$ ×2	3.181(9)
$Me1-S3^{4,6}$ ×2	2.824(7)
$Me1-S4A^{1}$	3.331(12)
$Me1-S4B^{1}$	3.734(12)
Mean	3.188
Vol.	55.91

TABLE 3 (*contd*.).

Me2A−S2A[1,8] ×2	2.941(11)	*Me2B*−S2B[1,9] ×2	2.964(11)
Me2A−S5A[4,6,11,12] ×4	2.938(7)	*Me2B*−S5B[4,6,13,14] ×4	2.947(7)
Mean	2.939	Mean	2.953
S2A[5]−*Me2A*−S5A	90.1(3)	S2B−*Me2B*−S5B	88.6(3)
S2A−*Me2A*−S5A	89.9(3)	S2B−*Me2B*−S5B	91.4(3)
S5A−*Me2A*−S5A	89.4(3)	S5B−*Me2B*−S5B	89.0(3)
S5A−*Me2A*−S5A	90.6(3)	S5B−*Me2B*−S5B	91.0(3)
Vol.	33.84	Vol.	34.30
OAV	0.15	OAV	1.69
Me3A−S2A[4,6] ×2	2.969 (7)	*Me3B*−S2B[4,6] ×2	3.013(7)
Me3A−S4A[1]	3.101 (11)	*Me3B*−S4B[1]	3.012(12)
Me3A−S5A[8]	2.917 (12)	*Me3B*−S5B[9]	2.984(11)
Me3A−S5A'[4,6] ×2	2.926 (7)	*Me3B*−S5B[4,6] ×2	2.895(7)
Mean	2.968	Mean	2.968
S2A−*Me3A*−S2A	88.2(3)	S2B−*Me3B*−S2B	86.6(3)
S2A−*Me3A*−S4A	90.7(3)	S2B−*Me3B*−S4B	91.9(3)
S2A−*Me3A*−S5A	89.8(3)	S2B−*Me3B*−S5B	89.7(3)
S2A−*Me3A*−S5A	90.9(2)	S2B−*Me3B*−S5B	91.1(2)
S4A−*Me3A*−S5A	92.5(3)	S4B−*Me3B*−S5B	90.5(3)
S5A−*Me3A*−S5A	89.8(3)	S5B−*Me3B*−S5B	91.1(3)
S5A−*Me3A*−S5A	87.1(3)	S5B−*Me3B*−S5B	88.0(3)
Vol.	34.82	Vol.	34.83
OAV	3.18	OAV	2.81
Me4A−S1A[5,7] ×2	2.833(7)	*Me4B*−S1B[5,7] ×2	2.879(8)
Me4A−S2A[1]	3.095(7)	*Me4B*−S2B[1]	3.078(11)
Me4A−S3[1]	2.637(11)	*Me4B*−S3[1]	2.809(9)
*Me4*A−S4A[5,7] ×2	2.967(7)	*Me4B*−S4B[5,7] ×2	3.036(8)
Mean	2.889	Mean	2.953
S1A−*Me4A*−S1A	93.6(3)	S1B−*Me4B*−S1B	91.7(4)
S1A−*Me4A*−S2A	85.6(3)	S1B−*Me4B*−S2B	84.8(3)
S1A−*Me4A*−S4A	88.9(2)	S1B−*Me4B*−S3	98.8(3)
S1A−*Me4A*−S3	96.3(3)	S1B−*Me4B*−S4B	91.0(2)
S2A−*Me4A*−S4A	90.8(3)	S2B−*Me4B*−S4B	90.2(3)
S4A−*Me4A*−S4A	88.3(3)	S4B−*Me4B*−S4B	85.8(3)
S3−*Me4A*−S4A	87.1(3)	S3−*Me4B*−S4B	86.0(3)
Vol.	31.95	Vol	34.00
OAV	14.17	OAV	24.00
Me5A−S1A[10]	2.701(11)	*Me5B*−S1B[1]	2.666 (11)
Me5A−S2A[5,7] ×2	2.922(7)	*Me5B*−S2B[5,7] ×2	2.899 (7)
Me5A−S4A[5,7] ×2	2.891(7)	*Me5B*−S4B[5,7] ×2	2.808 (8)
Me5A−S5A[1]	3.181(12)	*Me5B*−S5B[1]	3.162 (11)
Mean	2.918	Mean	2.874
S1A−*Me5A*−S2A	91.6(3)	S1B−*Me5B*−S2B	92.4(3)
S1A−*Me5A*−S4A	91.1(3)	S1B−*Me5B*−S4B	92.7(3)
S2A−*Me5A*−S2A	90.0(3)	S2B−*Me5B*−S2B	90.9(3)
S2A−*Me5A*−S4A	89.3(2)	S2B−*Me5B*−S4B	86.9(2)
S2A−*Me5A*−S5A	85.8(3)	S2B−*Me5B*−S5B	85.8(3)
S4A−*Me5A*−S4A	91.2(3)	S4B−*Me5B*−S4B	94.7(3)
S4A−*Me5A*−S5A	91.5(3)	S4B−*Me5B*−S5B	89.1(3)
Vol.	33.07	Vol.	31.50
OAV	4.44	OAV	9.52

Symmetry codes: [1] *x, y, z*; [2] *x, y*−1, *z*; [3] *x, y*+1, *z*; [4] *x*−½, *y*−½, *z*; [5] *x*+½, *y*−½, *z*; [6] *x*−½, *y*+½, *z*; [7] *x*+½, *y*+½, *z*; [8] −*x*+1, −*y*, −*z*; [9] −*x*+1, −*y*, −*z*+1; [10] *x*+1, *y*, *z*; [11] −*x*+3⁄2, −*y*−½, −*z*; [12] −*x*+3⁄2, −*y*+½, −*z*; [13] −*x*+3⁄2, −*y*−½, −*z*+1; [14] −*x*+3⁄2, −*y*+½, −*z*+1
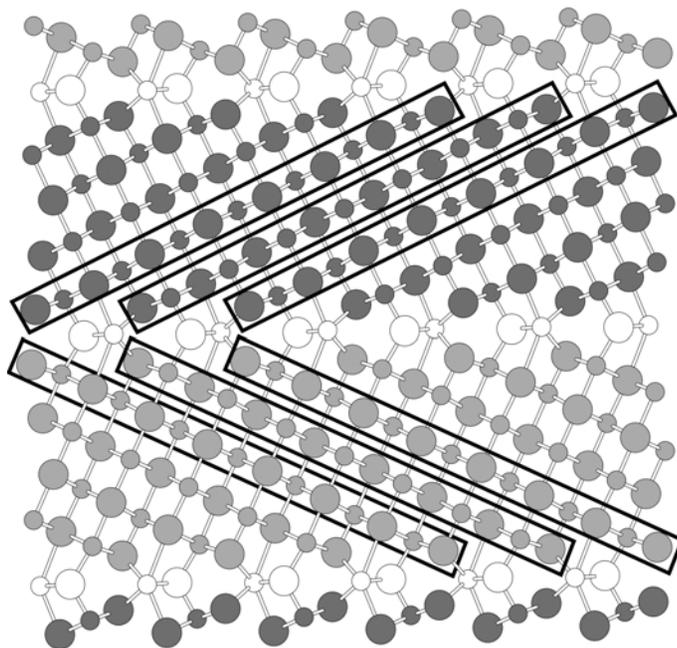
FIG. 2. A simplified sketch of the structure of ^{7,7}L lillianite homologues (small circles = *Me* sites; large circles = S sites). The alternate sets of (311)$_{PbS}$-like modules are evidenced by using different grey levels and in aschamalmite they are not mirror related. The rectangular boxes surround the layers of seven octahedra that converge towards the intermediate *Me1* sites (small empty circles).

in aschamalmite, connect adjacent octahedral layers *via* the common S3 vertex.

The lowering of symmetry in aschamalmite is ascribed to geometrical differences between A- and B-type octahedral slabs.

Pseudo-mirror related couples of the middle portions of the slabs exhibit similar geometries: <Me2A-S> 2.94 Å, <Me2B-S> 2.95 Å; both <Me3A-S> and <Me3B-S> 2.97 Å and all these octahedra have features compatible with a pure Pb population (<Pb-S> galena 2.97 Å; Wyckoff, 1963).

On the other hand, the polyhedra at the marginal portion of the octahedral layers form pseudo-mirror related couples, having different geometrical features from each other: a smaller Me4A octahedron (<Me4A-S> 2.89 Å) is opposed to a larger Me4B one (<Me4B-S> 2.95 Å); a larger Me5A octahedron (<Me5A-S> 2.92 Å) is opposed to a smaller Me5B one (<Me5B-S> 2.87 Å). These octahedra are also the most distorted in the structure (see for instance the OAV values in Table 3).

Distortion is a common feature of Pb and Bi polyhedra in sulphosalts due to the variable activity of the lone electron pair. This often masks the expected variation in the mean geometrical features that should enable the discrimination between $^{[VI]}Bi^{3+}$ and $^{[VI]}Pb^{2+}$, whose ionic radii are 1.03 and 1.19 Å, respectively (Shannon, 1976). It is known that the shorter distances of Pb and Bi polyhedra are less affected by the lone pair effects (Hummel and Armbruster, 1987) and a graph with the mean value of the three shortest distances plotted *vs.* the mean value of the next two shorter ones can be useful to identify Bi or Pb sites, because the existing fields for pure Pb and Bi polyhedra in sulphosalts are known (Hummel and Armbruster, 1987; Armbruster and Hummel, 1987).

Figure 4 shows that the *Me1*, *Me3B* and *Me4B* sites fit into the Pb field and that the *Me4A* and *Me5B* fit into the Bi field. All the other sites lie outside both fields, i.e. they exhibit features of polyhedra with a mixed Pb-Bi population.

This comparison produces further evidence for a greater similarity between the pseudo-mirror-related couples of the central portion of the slabs (Me2A-Me2B and Me3A-Me3B), whose points
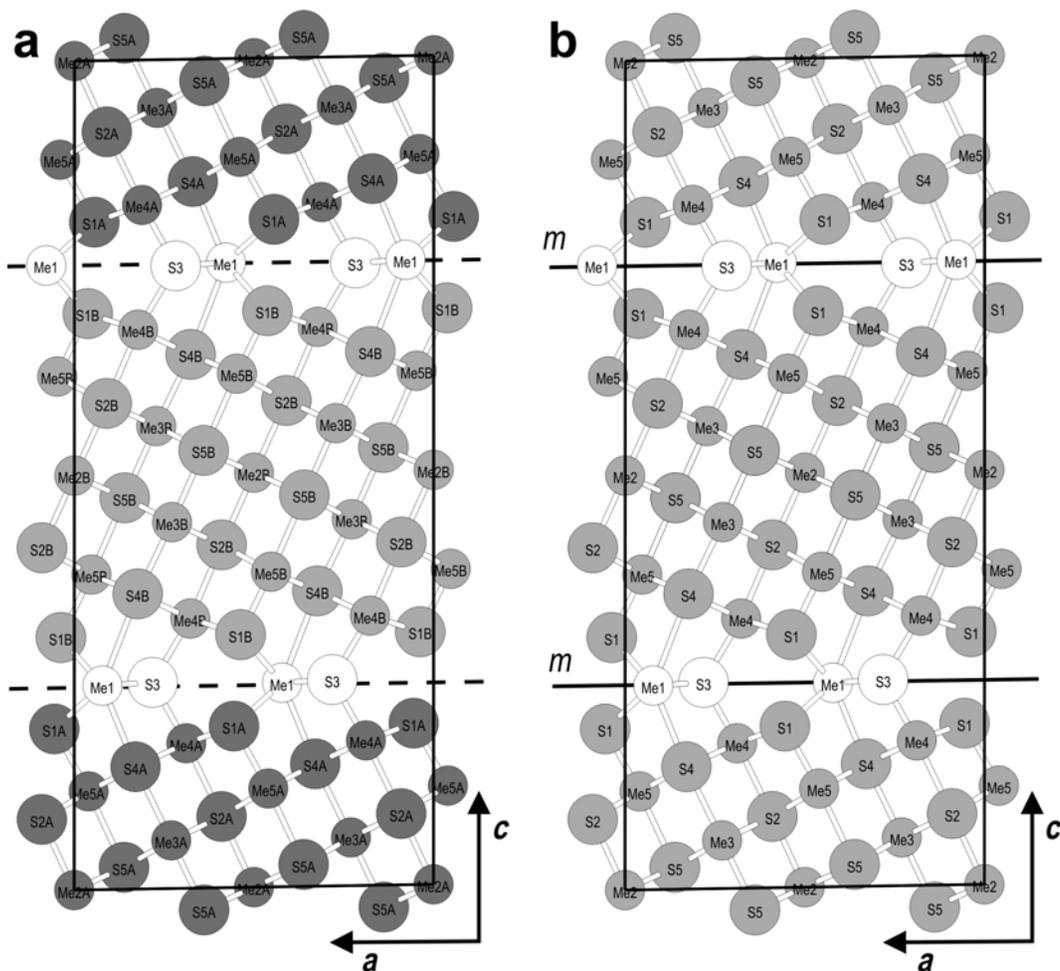
FIG. 3. (010) section of the unit cell of aschamalmite (*a*) and heyrovskyite (*b*). The absence of the (001) mirror plane in aschamalmite produces pseudo-mirror related slabs formed by non-equivalent octahedra (drawn with different grey levels).

are close each other, and strong differences for the marginal octahedral couples, in particular for the Me4A-Me4B one.

Site population in aschamalmite

Geometrical evidence suggests a different ordering of Pb and Bi among the marginal pseudo-mirror-related octahedral couples. In the past, many authors have attempted to solve this problem either on the basis of individual criteria (Kupčik, 1984), or by using the observed bond lengths (Berry, 1965; Armbruster and Hummel, 1987). More recently, the site population in

sulphosalts has been assigned by analysing the parameters of the circumscribed sphere, least-square fitted to the cation polyhedron (Balić-Žunić and Makovicky, 1996; Makovicky and Balić-Žunić, 1998; Makovicky *et al*., 2001).

We have used the *IVTON* software (Balić-Žunić and Vicković, 1996) to analyse the geometries of the Me polyhedra and selected parameters are reported in Table 4. Some values, such as the volume-based eccentricity Δ or the volume-based distorsion υ confirm that marginal octahedra are among the most distorted poly-hedra; in particular, the marginal octahedra have Δ values significantly greater than others.

TABLE 4. Coordination parameters for cation positions in the structure of aschamalmite and site occupancies calculated from Vs.

	CN	Vs (Å^3)	υ	Δ	σ	Occupancy
Me1	8	135.53	0.0484	0.1367	0.7421	1.00 Pb
Me2A	6	106.31	0.0001	0	0.9983	0.76 Pb + 0.24 Bi
Me2B	6	107.85	0.0007	0.0001	0.9911	0.86 Pb + 0.14 Bi
Me3A	6	109.84	0.0042	0.0954	0.9699	1.00 Pb
Me3B	6	109.64	0.0020	0.0815	0.9755	0.99 Pb + 0.01 Bi
Me4A	6	101.04	0.0066	0.2423	0.9808	0.39 Pb + 0.61 Bi
Me4B	6	107.45	0.0060	0.1751	0.9934	0.84 Pb + 0.16 Bi
Me5A	6	104.39	0.0048	0.2281	0.9840	0.62 Pb + 0.38 Bi
Me5B	6	99.32	0.0035	0.2453	0.9671	0.27 Pb + 0.73 Bi

Vs = volume of the circumscribed sphere, υ = volume-based distorsion, Δ = volume-based eccentricity, σ = volume sphericity

We then considered the eightfold coordinated *Me1* site completely filled with Pb. The occupancy of the octahedral sites has been assigned on the basis of the volume of the circumscribed sphere (Vs). The observed Vs values have been assumed as a linear relation between the values for pure Pb

TABLE 5. Bond-valence arrangement in aschamalmite.

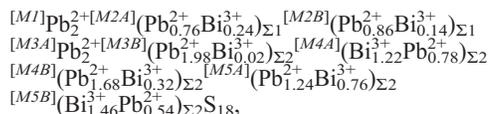| Site / Cation site valence[1]	*Me1* 2.00	*Me2A* 2.24	*Me2B* 2.14	*Me3A* 2.00	*Me3B* 2.01	*Me4A* 2.61	*Me4B* 2.16	*Me5A* 2.38	*Me5B* 2.73	Anion site valence[2]
S1A	0.17↓×2 →×2					0.47↓×2 →×2	0.68			1.96
S1B	0.18↓×2 →×2						0.42↓×2 →×2	0.73		1.93
S2A		0.35↓×2		0.32↓×2 →×2	0.23			0.37↓×2 →×2		1.96
S2B			0.33↓×2		0.29↓×2 →×2	0.24			0.40↓×2 →×2	1.95
S3	0.48↓×2 →×2					0.80	0.50			2.26
S4A	0.12			0.23		0.33↓×2 →×2	0.41×2 →×2			1.83
S4B	0.04				0.29	0.27↓×2 →×2			0.51↓×2 →×2	1.89
S5A		0.36↓×4 →×2		0.36↓×3 →×3				0.19		1.99
S5B			0.35↓×4 →×2		0.37↓×3 →×3				0.19	2.00
Cation site valence[2]	1.82	2.14	2.06	1.95	1.98	2.63	2.12	2.43	2.74	

Calculated after Brown and Altermatt (1985) with the parameters given by Brese and O'Keeffe (1991). The bond-valence analysis is charge-balanced only if the site multiplicity in taken into account (i.e. all the atom sites, except *Me2A* and *Me2B*, occur twice).

[1] calculated from assigned site population reported in Table 4.
[2] calculated from bond valence analysis.

and for pure Bi octahedra: the value chosen for Pb (109.84 $\mathring{A}^3$) corresponds to the largest Vs value in aschamalmite which is very similar to other pure PbS_6 octahedra (e.g. 110.51 $\mathring{A}^3$ in neyite; Makovicky *et al.*, 2001); the value for Bi (95.34 $\mathring{A}^3$) is that of BiS_6 octahedra in neyite and does not appear to be present among the octahedra in aschamalmite. The calculated occupancies are reported in Table 4 and a bond-valence analysis has been performed to validate the proposed site populations. The bond-valence parameters for Bi−S and Pb−S bonds being the same at 2.55 (Brese and O'Keeffe, 1991), a straightforward determination of occupancies is possible from the calculated valence-sums for cation positions.

The results shown in Table 5 are satisfactory and confirm the proposed site populations. In particular, in contrast with what the diagram in Fig. 4 suggests, in aschamalmite, pure Bi octahedra seem to be absent. On the basis of the assigned site populations, the crystal chemical formula of aschamalmite is:

$$^{[M1]}Pb_2^{2+}{}^{[M2A]}(Pb_{0.76}^{2+}Bi_{0.24}^{3+})_{\Sigma1}{}^{[M2B]}(Pb_{0.86}^{2+}Bi_{0.14}^{3+})_{\Sigma1}$$
$$^{[M3A]}Pb_2^{2+}{}^{[M3B]}(Pb_{1.98}^{2+}Bi_{0.02}^{3+})_{\Sigma2}{}^{[M4A]}(Bi_{1.22}^{3+}Pb_{0.78}^{2+})_{\Sigma2}$$
$$^{[M4B]}(Pb_{1.68}^{2+}Bi_{0.32}^{3+})_{\Sigma2}{}^{[M5A]}(Pb_{1.24}^{2+}Bi_{0.76}^{3+})_{\Sigma2}$$
$$^{[M5B]}(Bi_{1.46}^{3+}Pb_{0.54}^{2+})_{\Sigma2}S_{18},$$

which corresponds to the uncharge-balanced unit formula $Pb_{5.92}Bi_{2.08}S_9$, very close to the stoichiometric unit formula $Pb_6Bi_2S_9$. The residual charge (+0.08) suggests a small inaccuracy on the polyhedral dimension chosen for pure Pb and pure Bi.

Discussion

This study reveals that the monoclinic symmetry of aschamalmite originates from Pb-Bi ordering that occurs in two alternating sets of octahedral slabs. When both layers show the same cation distributions, the structure is orthorhombic and the two sets of layers are related by the (001) mirror plane passing through the *Me1* bicapped trigonal prisms. In this case, the layers are defined only by 4 independent octahedra and the structure is that of the ^{7,7}L homeotype heyrovskyite.

In aschamalmite, the independent octahedra total eight and the two alternating sets of layers are related by a pseudo-mirror plane passing through *Me1* sites. In particular, the inner portions of the two octahedral slabs show similar features, conforming to Pb octahedra in sulphosalts: *Me3A* and *Me3B* sites are pure Pb polyhedra whereas the
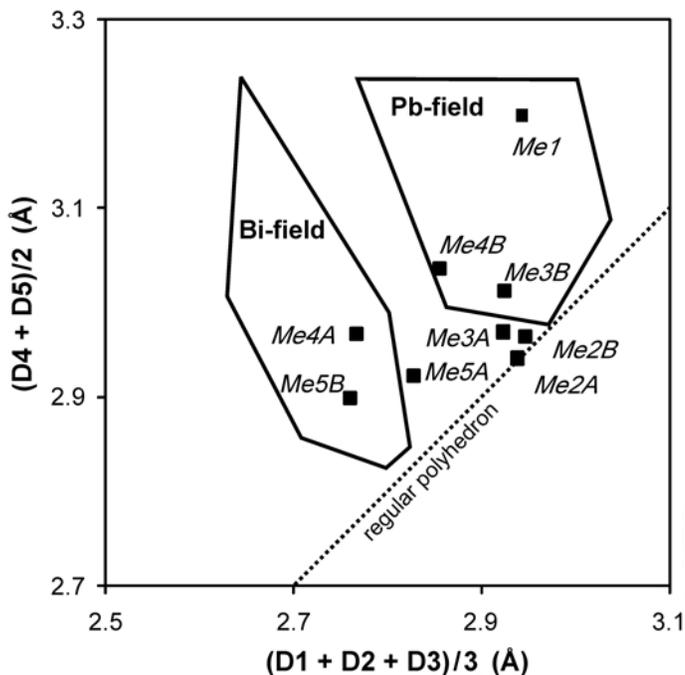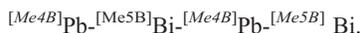

FIG. 4. Shortest three *Me*−S distances plotted *vs.* the next two shorter ones for *Me* sites in aschamalmite. A complete ordering does not occur because several sites lie outside the Pb and Bi-fields.

geometries and the calculated valences for $Me2A$ and $Me2B$ sites suggest the presence of a minor Bi content. This results in the central portion of the aschamalmite structure hosting three of the six Pb a.p.f.u. On the contrary, the marginal portion of the two octahedral slabs show different features: $Me4A$ contains a dominant Bi population while $Me4B$ shows a major Pb content; $Me5A$ predominantly hosts Pb while $Me5B$ contains a predominance of Bi.

Therefore, the cation-ordering scheme in aschamalmite is consistent with the alternation between Pb and Bi octahedra in the margin of the octahedral slabs and the two sets of layers result with an opposite ordering scheme: when the layer formed by A polyhedra shows the succession
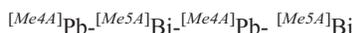
$$^{[Me4A]}\text{Bi-}^{[Me5A]}\text{Pb-}^{[Me4A]}\text{Bi-}^{[Me5A]}\text{Pb,}$$
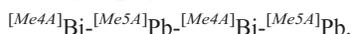
the layer formed by B polyhedra shows the opposite series

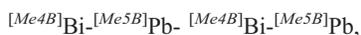$$^{[Me4B]}\text{Pb-}^{[Me5B]}\text{Bi-}^{[Me4B]}\text{Pb-}^{[Me5B]}\text{Bi.}$$

This structural arrangement corresponds to two Pb a.p.f.u. and two Bi a.p.f.u., in agreement with the stoichiometry of aschamalmite. This ordering probably allows more efficient local charge balance on anion sites, in particular on anions bonded to Me1, that hosts the remaining Pb a.p.f.u. and connects the margins of A and B octahedral layers.
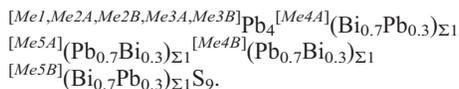
It is clear also that an opposite situation, in which the alternation

$$^{[Me4A]}\text{Pb-}^{[Me5A]}\text{Bi-}^{[Me4A]}\text{Pb-}\,^{[Me5A]}\text{Bi}$$

is faced to the series

$$^{[Me4B]}\text{Bi-}^{[Me5B]}\text{Pb-}\,^{[Me4B]}\text{Bi-}^{[Me5B]}\text{Pb,}$$

can provide the same local arrangement. The aschamalmite studied shows 70% of its unit cells in agreement with the first ordering scheme while the remaining unit cells have the opposite ordering scheme, resulting in a simplified crystal-chemical formula:

$$^{[Me1,Me2A,Me2B,Me3A,Me3B]}\text{Pb}_4{}^{[Me4A]}(\text{Bi}_{0.7}\text{Pb}_{0.3})_{\Sigma 1}$$
$$^{[Me5A]}(\text{Pb}_{0.7}\text{Bi}_{0.3})_{\Sigma 1}{}^{[Me4B]}(\text{Pb}_{0.7}\text{Bi}_{0.3})_{\Sigma 1}$$
$$^{[Me5B]}(\text{Bi}_{0.7}\text{Pb}_{0.3})_{\Sigma 1}\text{S}_9.$$

Nevertheless, this formula could also be due to the presence of a (100) pseudo-merohedral twinning of two completely ordered portions, formed by pure-populated octahedra, in the ratio 70:30. It is difficult to detect this pseudo-merohedral twinning experimentally when the monoclinic angle is close to 90º. We have checked the presence of twinning, assuming the twin-law matrix $(100, 0\bar{1}0, 00\bar{1})$ during the structure refinement of a completely ordered model. The relative abundance of the second component converges to 0.02(2)%, and for this motif we have excluded the presence of twinning in the crystal investigated in this study.

Aschamalmite is characterized by a short-range order on the unit-cell scale, with the features described above. If the two opposite ordering schemes occur in the same percentage and are statistically distributed, the crystal structure changes to the orthorhombic form and both the marginal $Me4$ and $Me5$ sites are half-populated by Pb and Bi.

At far as we know, this is not the case for heyrovskyites studied to date which are considered to have the $Me5$ site fully Bi-populated. However, the structural data available are for natural heyrovskyite which always contains monovalent Ag (positioned in the Me4 octahedron) and which therefore requires a greater Bi content (total Bi >2 a.p.f.u.). This makes it difficult to draw a direct comparison with our stoichiometric aschamalmite. It would be interesting to know the cation distributions of stoichiometric heyrovskyite ($\text{Pb}_6\text{Bi}_2\text{S}_9$) and to confirm the population at the $Me4$ and $Me5$ sites. If the $Me4$ and $Me5$ sites do have a mixed Pb-Bi population, the ordering rule proposed for aschamalmite is probably true for both the ^{7,7}L lillianite homologues.

On the other hand, there is no crystallographic reason which prevents the formation of a completely ordered aschamalmite in which only one ordering scheme occurs for all the unit cells forming the crystal. This hypothetical phase would show only pure-populated octahedral sites, with a regular change of Pb and Bi at the marginal sites (e.g. $^{[Me4A]}\text{Bi}$, $^{[Me4B]}\text{Pb}$, $^{[Me5A]}\text{Pb}$, $^{[Me5B]}\text{Bi}$). In respect of the aschamalmite studied in this work, the completely ordered phase should have a more evident monoclinic distortion. However, aschamalmites having a high monoclinic β angle have yet to be reported.

It is known that, at ambient pressure conditions, aschamalmite is not stable in the system PbS-PbSe-Bi_2S_3-Bi_2Se_3 at 500ºC (Liu and Chang, 1994). This assumption has recently been confirmed by the discovery of heyrovskyite in the fumaroles of Vulcano, Aeolian Islands, Italy, where a temperature close to 500ºC was measured. Heyrovskyite is also present in deposits formed at 350−400ºC (Makovicky *et al.*, 1991)

and only at temperature below these values can aschamalmite form, first as a partly ordered phase and then as a completely ordered phase. The rarity of aschamalmite in the lithosphere is probably due to the uncommon *P-T* conditions required to crystallize the $Pb_6Bi_2S_9$ compound in the monoclinic form.

Acknowledgements

References

Altomare, A., Burla, M.C., Camalli, M., Cascarano, G.L., Giacovazzo, C., Guagliardi, A., Moliterni, A.G.G., Polidori, G. and Spagna, R. (1999). SIR97: a new tool for crystal structure determination and refinement. *Journal of Applied Crystallography*, **32**, 115−119.

Armbruster, T. and Hummel, W. (1987) (Sb,Bi,Pb) ordering in sulfosalts: Crystal-structure refinement of a Bi-rich izoklakeite. *American Mineralogist*, **72**, 821−831.

Balestra, C. and Armellino, G. (2001) La miniera di Costabella. *Notiziario di mineralogia del Ferrania Club*, **15**, 20−26.

Balić-Žunić, T. and Vicković, I. (1996) IVTON − Program for the calculation of geometrical aspects of crystal structures and some crystal chemical applications. *Journal of Applied Crystallography*, **29**, 305−306.

Balić-Žunić, T. and Makovicky, E. (1996) Determination of the centroid or 'the best centre' of a coordination polyhedron. *Acta Crystallographica B*, **52**, 78−81.

Berry, L.G. (1965) Recent advances in sulfide mineralogy. *American Mineralogist*, **50**, 301−313.

Borodaev, Y.S., Garavelli, A., Garbarino, C., Grillo, S.M., Mozgova, N.N., Paar, W.H., Topa, D. and Vurro, F. (2003) Rare sulfosalts from Vulcano, Aeolian Islands, Italy. V. selenian heyrovskyite. *The Canadian Mineralogist*, **41**, 429−440.

Brese, N.E. and O'Keeffe, M. (1991) Bond-valence parameters for solids. *Acta Crystallographica B*, **47**, 192−197.

Brown, I.D. and Altermatt, D. (1985) Bond-valence parameters obtained from a systematic analysis of the inorganic crystal structure database. *Acta Crystallographica B*, **41**, 244−247.

Bruker (2003). *SAINT Software Reference Manual. Version 6*. Bruker AXS Inc., Madison, Wisconsin, USA.

Busing, W.R., Martin, K.O. and Levy H.A. (1962) *Orfls. Report Ornl-Tm-305.- Oak Ridge, Tn*: Oak Ridge Natl. Lab. Tennessee, USA.

Callegari, A., Boiocchi, M. and Cech, G. (2008) Ritrovamento di aschamalmite in Val di Susa, Piemonte. *Micro*, **1**, 125−128.

Hummel, W. and Armbruster, T. (1987) Tl^+, Pb^{2+}, and Bi^{3+} bonding and ordering in sulfides and sulfosalts. *Schweizerische Mineralogische und Petrographische Mitteilungen*, **67,** 213−218.

Kupčik, V. (1984) Die Kristallstruktur des Minerals Eclarit $(Cu,Fe)Pb_9Bi_{12}S_{28}$. *Tschermaks Mineralogische und Petrographische Mitteilungen*, **32**, 259−269.

Liu, H. and Chang, L.L.Y. (1994) Lead and bismuth chalcogenide system. *American Mineralogist*, **79**, 1159−1166.

Makovicky, E. (1977) Chemistry and crystallography of the lillianite homologous series. Part III. Related phases. *Neues Jahrbuch für Mineralogie Abhandlungen*, **131**, 187−207.

Makovicky, E. and Karup-Møller, S. (1977a) Chemistry and crystallography of the lillianite homologous series. Part. I: General properties and definitions. *Neues Jahrbuch für Mineralogie Abhandlungen*, **130**, 264−287.

Makovicky, E. and Karup-Møller, S. (1977b) Chemistry and crystallography of the lillianite homologous series. Part. II: Definition of new minerals: eskimoite, vikingite, ourayite and treasurite. Redefinition of schirmerite and new data on the lillianite-gustavite solid-solution series. *Neues Jahrbuch für Mineralogie Abhandlungen*, **131**, 56−82.

Makovicky, E. and Balić-Žunić, T. (1993) Contribution to the crystal chemistry of thallium sulphosalts. II TlSb3S5 − the missing link of the lillianite homologous series. *Neues Jahrbuch für Mineralogie Abhandlungen*, **165**, 331−344.

Makovicky, E. and Balić-Žunić, T. (1998) New measure of distortion for coordination polyhedra. *Acta Crystallographica B*, **54**, 766−773.

Makovicky, E., Mumme, W.G. and Hoskins, B.F. (1991): The crystal structure of heyrovskite. *The Canadian Mineralogist*, **29**, 553−559.

Makovicky, E., Balić-Žunić, T. and Topa, D. (2001) The crystal structure of neyite, $Ag_2Cu_6Pb_{25}Bi_{26}S_{68}$. *The Canadian Mineralogist*, **39**, 1365−1376.

Moëlo, Y., Makovicky, E., Mozgova, N.N., Jambor, J.L., Cook, N., Pring, A., Paar, W.H., Nickel, E.H.,

Graeser, S., Karup-Møller, S., Balić-Žunić, T., Mumme, W.G., Vurro, F., Topa, D., Bindi, L., Bente, K. and Shimizu, M. (2008) Sulfosalt systematics: a review. Report of the sulfosalt sub-committee of the IMA Commission on Ore Mineralogy. *European Journal of Mineralogy*, **20**, 7−46.

Mumme, W.G., Niedermayr, G., Kelly, P.R. and Paar, W.H. (1983) Aschamalmite $Pb_{5.92}Bi_{2.06}S_9$, from Untersulzbach Valley in Salzburg, Austria. *Neues Jahrbuch für Mineralogie Monatshefte*, 433−444.

Perchiazzi, N. (1989) Aschamalmite: secondo ritrovamento in natura presso l'Alpe Cedo, Val d'Ossola. *Rivista Mineralogica Italiana*, **4**, 238−240.

Shannon, R.D. (1976) Revised effective ionic radii and systematic studies of interatomic distances in halides and chalcogenides. *Acta Crystallographica A*, **32**, 751−767.

Sheldrick, G.M. (1996) *SADABS Siemens Area Detector Absorption Correction Program.* University of Göttingen, Germany.

Takeuchi, Y. and Takagi, J. (1974) The Structure of Heyrovskyite ($6PbS\cdot Bi_2S_3$). *Proceedings of the Japan Academy*, **50,** 76−79.

Wyckoff, R.W.G. (1963) Pp. 85−237 in: *Crystal Structures I. 2nd edition (rocksalt structure).* Interscience Publishers, New York.